Fractal corrosion of alloy films by acid

1990 J. Phys.: Condens. Matter 2 1971

(http://iopscience.iop.org/0953-8984/2/8/003)

J. Phys.: Condens. Matter **2** (1990) 1971–1975. Printed in the UK

Fractal corrosion of alloy films by acid

J R Ding and B X Liu†
Department of Materials Science and Engineering, Tsinghua University, Beijing 100084, People's Republic of China

Received 5 September 1989

Abstract. Fractal structures were observed during the corrosion of Ni–Mo alloy films by reactive acid. It was found that the corrosion time was a crucial point in forming the fractal acid-etched channels. The diffusion-limited aggregation model with consideration of the cumulative effect can explain the formation process of the observed fractal well. The multi-scaling properties of the observed fractals were also studied and showed some differences from those reported earlier.

It has been found that many physical phenomena, such as the self-similar branching structure in electrochemical deposition [1, 2] and diffusion-limited polymerisation [3], could result in fractal structures [4–7]. The diffusion-limited-aggregation (DLA) model [8, 9] has proved to be useful in the understanding of various fractal processes. However, the DLA model cannot describe many fractal phenomena in detail, and other models [10] based on the DLA model have been developed to explain various fractal structures that have resulted from real physical processes. In [11] a model based on the DLA model was proposed and the cumulative effect was taken into consideration. This model successfully described some physical processes, such as chemical dissolution of a porous medium by a reactive fluid [11], viscous fingering [12] and dielectric breakdown [13]. In this paper, we present an experimental result of two-dimensional fractal corrosion in thin alloy films by reactive acid which can be explained by the model in [11]. Furthermore, we present the multi-fractal properties of the fractals observed in this study using the method proposed in [14–17].

Firstly, multi-layered samples were prepared by electron gun evaporation of the pure metal Ni and Mo alternately onto substrates in a vacuum system. The substrates were oxidised silicon wafers, and the thickness of the oxidised layer (SiO_2) was about 500 nm. The vacuum level before evaporation was better than 5×10^{-8} Torr. The alloy films consisted of three layers of Ni and two layers of Mo. The thickness of each layer is exhibited in figure 1. After evaporation, the films were aged at room temperature for about one year. Figure 2 shows the depth profiles of Ni and Mo obtained by Rutherford back-scattering (RBS) analysis. A nearly uniform distribution is revealed, and this is attributed to the atom diffusion through the interfaces.

† Also at the Center of Condensed Matter and Radiation Physics, CCAST (World Laboratory), Beijing, People's Republic of China.

0953-8984/90/081971 + 05 $03.50

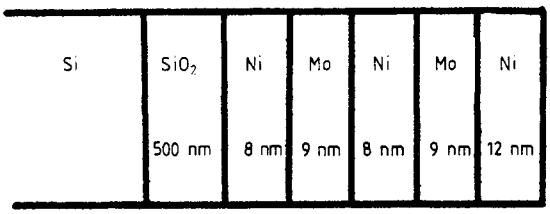

Figure 1. Schematic diagram of as-evaporated multi-layer samples. The thickness of each layer is shown.

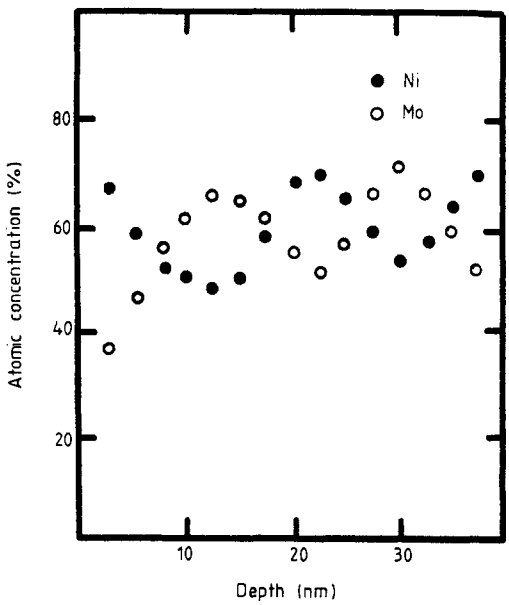

Figure 2. The depth profile (obtained from RBS analysis) of Ni and Mo after the multi-layered samples had been aged at room temperature for a year.

The aged samples were put into hydrofluoric acid. The samples floated on the hydrofluoric acid owing to the surface tension. The SiO_2 layer was corroded away rapidly in about the first 30 s by the acid, and then the acid corroded the alloy films from the back side. After having been corroded by hydrofluoric acid for various times, several alloy films were collected on Cu or Mo grids for transmission electron microscopy (TEM) examination. TEM examination and energy-dispersive spectroscopy (EDS) analysis revealed that there were many nickel-rich regions (black under bright-field examination) in the alloy films. The diameter of the nickel-rich regions was about 10 μm. Electron diffraction analysis revealed that the alloy films were a mixture of metal Ni and Mo, and no inter-metallic compound was detected.

Fractal patterns were observed in those samples which were corroded for a specific time period 1 min $< t <$ 15 min, while, for a corrosion time of either $t <$ 1 min or $t >$ 15 min, no fractal acid-etched pattern was observed. Since Ni was easier to corrode away than Mo by hydrofluoric acid when the corrosion time t was greater than 30 min, for the alloy films which contained mainly Mo (as confirmed by electron diffraction and EDS analyses) neither a Ni-rich region nor a fractal pattern was observed.

Figure 3(*a*) shows a typical bright-field image observed in a sample which was corroded for 3 min by hydrofluoric acid. The fractal dimension was determined to be 1.51 ± 0.02 by the box-counting method. This value was an average over several similar

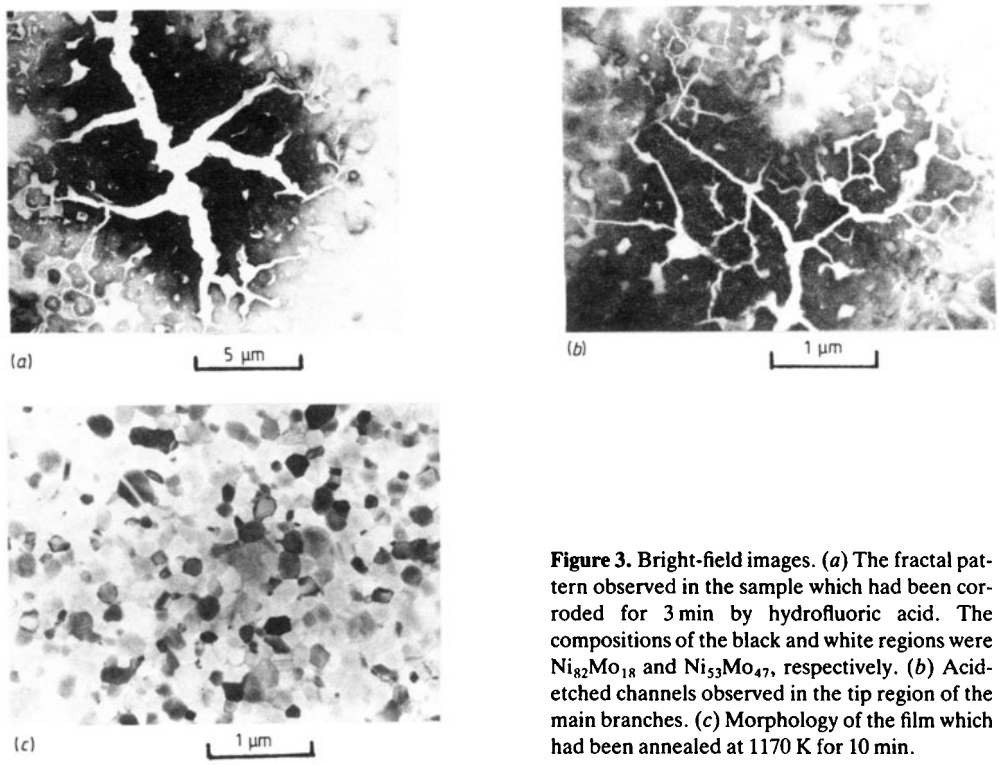

Figure 3. Bright-field images. (*a*) The fractal pattern observed in the sample which had been corroded for 3 min by hydrofluoric acid. The compositions of the black and white regions were $Ni_{82}Mo_{18}$ and $Ni_{53}Mo_{47}$, respectively. (*b*) Acid-etched channels observed in the tip region of the main branches. (*c*) Morphology of the film which had been annealed at 1170 K for 10 min.

fractal patterns. TEM examination revealed that every observed fractal pattern was centred at a nickel-rich region as mentioned above. EDS analysis showed that the compositions of black and white (acid-etched channel) regions in figure 3(*a*) were $Ni_{82}Mo_{18}$ and $Ni_{53}Mo_{47}$, respectively, while the composition of the matrix (the outside region) was determined to be $Ni_{46}Mo_{54}$. It is therefore concluded that the formation process of the fractal patterns is as follows. Firstly, after the SiO_2 layer had been corroded away, hydrofluoric acid began to corrode the alloy films. Since Ni is easier to corrode away than Mo, the hydrofluoric acid corroded the Ni-rich regions preferentially. This explained why each fractal pattern was centred at a Ni-rich region. Secondly, the corrosion developed in two directions, i.e. one proceeding outwards from the centre and the other broadening the acid-etched channels, corresponding to the so-called 'cumulative effect'. The fractal patterns observed in this study were very similar to those obtained from the model in [11], implying a similar underlying mechanism for the two cases.

Figure 3(*b*) shows a typical corrosion pattern observed in a tip region of a large etching channel. The corresponding compositions were almost the same as those mentioned above. Hence, all the three different zones reported in [11] were also clearly observed in our case. Figures 3(*a*) and 3(*b*) correspond to zones 1 and 2, and the matrix corresponds to zone 3. The radius $R < 5\ \mu m$ belonged to zone 1, $5\ \mu m < R < 10\ \mu m$ belonged to zone 2, and $R > 10\ \mu m$ was zone 3 (the matrix).

The thermal stability of the observed fractal patterns was also studied by TEM *in situ* annealing. The vacuum level was better than 5×10^{-6} Torr during annealing. *In situ* annealing revealed that the observed fractal patterns began to disappear at a temperature

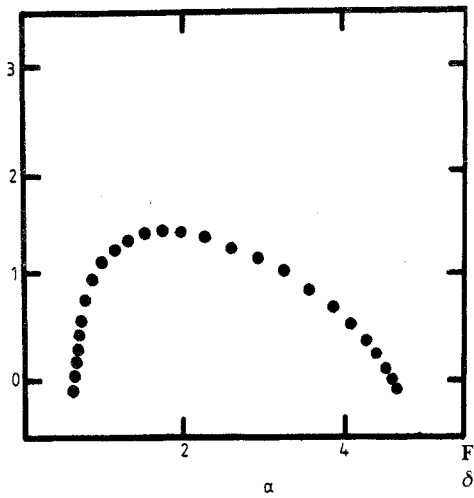

Figure 4. The f–α spectrum of the fractal with the interval $\delta q = 0.1$. The Laplacian potential gradient was used.

of 1170 K, since atom diffusion is easy at high temperatures. At this temperature, a phase transition took place. The new phase was identified as Ni_3Mo inter-metallic compound by electron diffraction. Figure 3(c) shows a bright-field image observed after annealing at this temperature.

In order to compare the scaling properties of the fractal structures observed in this study with those of other fractal structures, we calculated the generalised dimension $D(q)$ with q ranging from -10 to 10, as well as the f–α spectra. The Laplacian potential gradient was used. Firstly, the fractal patterns were put into a Laplacian field with the following conditions: the fractal pattern itself was an equipotential (the potential was set at zero), and the outer boundary was also an equipotential (the potential was set to unity); the diameter of the outer boundary was about three times that of the fractal structure. The Laplacian potentials were then calculated numerically according to the discrete Laplace equation. Let the growth probability of each growth point $P_g(x) \propto |\nabla_n \varphi_{(x)}|$. Use a set of boxes of size ε to cover the perimeter of the fractal structure, and let $P_i(\varepsilon)$ be the growth probability accumulated within the ith box of size ε. The generalised dimensions $D(q)$ and the f–α spectra were then calculated according to the following definitions:

$$D(q) = \lim_{(\varepsilon \to 0)} (q-1)^{-1} \log\left(\sum_i p_i(\varepsilon)^q\right) \Big/ \log \varepsilon \tag{1}$$

$$\alpha(q) = (\mathrm{d}/\mathrm{d}q)(q-1)D(q) \tag{2}$$

$$f(\alpha(q)) = q\alpha(q) - (q-1)D(q). \tag{3}$$

Figure 4 shows the f–α spectrum of the fractals observed in this study with the Laplacian potential gradient measure. The information dimension $D(1) = 1.2$, and the correlation dimension $D(2) = 0.83$. In the limit $q \to \infty$, $D(\infty) = \alpha(\infty) = 0.73$, which are considerably larger than those expected from the DLA model (0.64–0.70). On the other hand, in the limit $q \to -\infty$, $D(-\infty) = \alpha(-\infty) = 4.9$, which is considerably smaller than expected from the DLA model (about 9.0). This means that our f–α spectra have a relatively narrow range. Compared with the aggregates obtained from the DLA model [16], the fractals

observed in this study are relatively open and have a smaller screening effect. This shows that the cumulative effect modifies the DLA model significantly.

In conclusion, fractal patterns were observed when the Ni–Mo alloy films were corroded by hydrofluoric acid for a specific corrosion time period 1 min $< t <$ 15 min. The cumulative-effect-modified DLA model can explain the formation process of the fractals well. The fractals disappeared when the films were annealed at a temperature of 1170 K. Multi-fractal analysis showed that the fractals had a relatively narrow range of singularity α, implying that the underlying mechanism of the corrosion fractals was quite different from that of the DLA model.

Acknowledgments

The authors are grateful to Dr E Ma, Dr L J Huang and researchers of the TEM Laboratory of Beijing University and the Analysis Center of Tsinghua University for their help. The partial financial aid from the International Atomic Energy Agency under Contract 4731/RB is also acknowledged. This project was supported by the National Natural Science Foundation of China.

References

[1] Matsushita M, Sano M, Hayakawa Y, Honjo H and Sawada Y 1984 *Phys. Rev. Lett.* **53** 286
[2] Brady R M and Ball R C 1984 *Nature* **309** 225
[3] Kaufmann, Daccord G and Stanley H E 1985 *Nature* **314** 141
[4] Family F and Landau D P (ed) 1984 *Kinetics of Aggregation and Gelation* (Amsterdam: North-Holland)
[5] Stanley H E and Ostrowsky N (ed) 1985 *On Growth and Form* (The Hague: Nijhoff)
[6] Pietronero L and Tosatti E (ed) 1986 *Fractals in Physics* (Amsterdam: North-Holland)
[7] Mandelbrot B B 1982 *The Fractal Geometry of Nature* (San Francisco, CA: Freeman)
[8] Witten T A and Sander L M 1981 *Phys. Rev. Lett.* **47** 1400
[9] Witten T A and Sander L M 1983 *Phys. Rev.* B **27** 5686
[10] Voss R F 1984 *J. Stat. Phys.* **36** 861
[11] Daccord G 1987 *Phys. Rev. Lett.* **58** 479
[12] Paterson L 1984 *Phys. Rev. Lett.* **52** 1621
[13] Niemeyer L, Pietronero L and Wiesmann H J 1984 *Phys. Rev. Lett.* **52** 1033
[14] Halsey T C, Jensen M H, Kadanoff L P, Procaccia I and Shraiman B I 1986 *Phys. Rev.* A **33** 1141
[15] Ohta S and Honjo H 1988 *Phys. Rev. Lett.* **60** 611
[16] Hayakawa Y, Sato S and Matsushita M 1987 *Phys. Rev.* A **36** 1963
[17] Meakin P, Coniglio A and Stanley H E 1986 *Phys. Rev.* A **34** 3325